Automatic Extraction of 3D Nuclear Bounding Surfaces from CLSM Imagery of Developing *Arabidopsis* Flowers

M.C. Burl[1], A.H.K. Roeder[2], C.K. Ohno[2], E.D. Mjolsness[3,1], E.M. Meyerowitz[2]

[1]Jet Propulsion Laboratory, California Institute of Technology,

[2]California Institute of Technology, Division of Biology,

[3]University of California at Irvine, Department of Information and Computer Science

Abstract

As part of the Computable Plant Project[1]*, we are using Confocal Laser Scanning Microscopy (CLSM) to help build computational models of development in* Arabidopsis*. The computational models are intended to capture the key processes involved in plant development over a range of scales from sub-cellular to whole-organism. CLSM provides non-destructive* in vivo *imaging at multiple optical depths to capture specific structures that have been fluorescently labeled, such as plasma membranes, cell nuclei, and the expression patterns of individual genes. In support of the modeling activities, we have developed an algorithm that automatically extracts triangulated mesh models of nuclear bounding surfaces from CLSM image stacks.*

1. Introduction

All multicellular organisms arise from a single cell. A great mystery in biology is how the descendants of this cell differentiate to form the many distinct cell types that carry out the complex functions of each organ. We are addressing this question in flowers of the model plant, *Arabidopsis thaliana*.

The sepals are the outermost floral organs, which cover and protect the flower while it develops and open when the flower blooms at maturity. We have known for more than a decade that the transcription factors APETALA1 and APETALA2 specify sepal organ identity but we still do not know how they regulate the downstream processes controlling cell division, cell expansion, and cell fate specification that actually generate the sepal [3,6,1,4]. The sepal epidermis contains a complex pattern of cells including greatly enlarged giant cells apparently randomly interspersed between smaller epidermal cells, hairs (trichomes), and guard cells (which form the stomatal pores for gas exchange). The presence of giant cells and smaller cells suggests that there is differential regulation of cell division and/or cell expansion between the epidermal cells and raises several questions. Do the giant cells form because they merely stop dividing earlier than their smaller neighbors, but continue to expand? Do the giant cells expand faster than their smaller neighbors?

To address these questions, living cells in the developing sepal epidermis must be observed to determine the expansion rate and the lineage of cells that produce giant cells versus smaller epidermal cells. Achieving this goal requires the development of new methods for analyzing 3D time-lapse image stacks that can be acquired with confocal laser scanning microscopy (CLSM). Although identification of nuclei in an image stack can be done by hand, it is a time-consuming process, which can only be completed on a small number of samples. An automated approach is, therefore, necessary to enable the analysis of sufficient specimens to provide statistically significant data.

[1]`http://www.computableplant.org/`

2. CLSM Data Collection

CLSM has been used previously to image the meristem of living plants [8], and we have adapted this technique to image developing sepals with a Zeiss 510 meta confocal microscope. The sepal epidermis is visualized with a nuclear-localized cyan fluorescent protein (CFP) expressed exclusively in the epidermal cell layer (*ML1::2XCFP-N7*) and the lipophilic fluorescent dye FM4-64, which labels the plasma membranes. The result is a stack of images at approximately 2 μm depth increments. Figure 1a shows an *Amira* volume rendering of a CLSM image stack.

3. Algorithm

From an image stack, $\mathbf{I}$, we want to automatically extract 3D triangulated mesh models that describe the nuclear bounding surfaces. A specific voxel within $\mathbf{I}$ is indexed by integral coordinates $[x, y, z]$, where z measures depth along the optical axis[2]. The data is arranged by image frames, where a frame is a slice through the stack at a specific z-value. Our algorithm consists of the following steps: smoothing, contour detection within each frame, z-linking, and mesh generation.

Smoothing: To improve signal-to-noise ratio, smoothing is employed in both the z direction (across stack levels) and in the (x, y) directions (within a single stack level). The z-smoothing is accomplished by averaging an image frame with the two adjacent frames, while the (x, y)-smoothing is accomplished using a discrete analog of the 2D-Gaussian filter as in [5].

Contour Detection: After smoothing, a contour detection algorithm is applied independently to each frame in the smoothed stack. We have experimented with several contour detection approaches [2,5,9,7]. All of these local detectors produce some spurious segments that must be eliminated. In the experiments reported in Section 4, we used a technique similar to [2] with two additional validation tests: (1)

[2]Smaller z values are at the *top* of the stack (closer to the microscope) and larger z values are at the bottom of the stack.

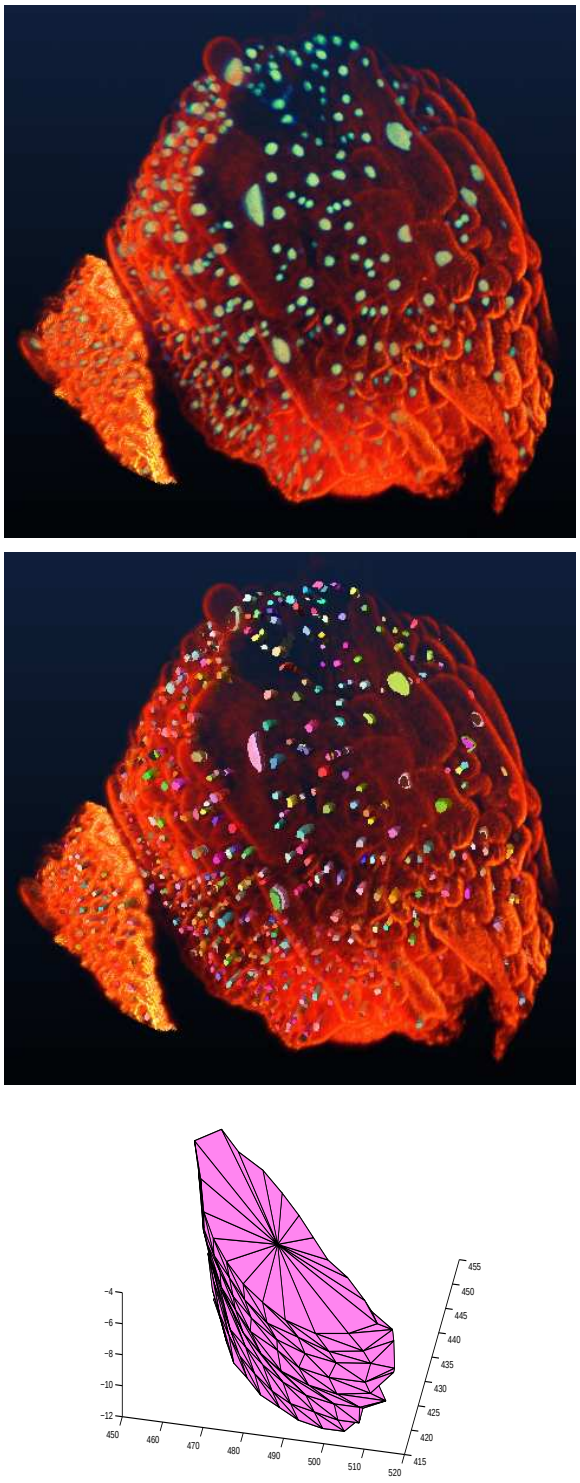

Figure 1: (a) *Amira* volume rendering of a CLSM image stack taken through a developing *Arabidopsis* flower. Cell nuclei are labeled with a nuclear localized cyan fluorescent protein (CFP) displayed in the green channel, while the plasma membrane at the cell periphery is stained with FM4-64, which is displayed in the red channel. (b) Superposition of the extracted 3D nuclear bounding surfaces with the red (membrane) channel. (c) Triangulated mesh modeling the 3D structure of one of the giant cell nuclei.

a length test to reject short contours due to nosie and (2) a closure test to reject any contours that are not approximately closed. The end result is a set of contours at each stack level.

z-Linking: The next step is to link contours across stack levels. For a given stack level, the linking algorithm visits each contour. If a contour is unlabeled, it receives a new label. The algorithm also checks the next stack level to see if a contour there matches with the current contour. If so, the matching contour at level $z+1$ receives the same label as the current contour. The determination of whether two contours "match" is based on a measure of contour dissimilarity. The dissimilarity is computed based on the distance between corresponding points on two contours after they have been aligned by resampling, shifting, and varying the curve sense[3]

Triangulation: After z-linking, each contour is associated with an integer label such that linked contours have the same label. The final step is to derive a triangulated mesh for the surface of each object. Contours within an object are resampled and aligned as in the previous section. Consider an object consisting of two (aligned) contours each with p sample points. The surface area between the two can be triangulated with $2p$ triangles, e.g., $\{i, i-1, j-1\}$ and $\{i, j-1, j\}$ for $i = 1, \ldots p$ and $j = i$, where i is the contour index on the upper contour and j is the contour index on the lower contour. For the top and bottom surfaces, we assume star convexity with respect to the center of mass of the face vertices, which allows a simple triangulation with p triangles on each face. Thus, the complete triangulation of an object with L levels requires $2Lp$ triangles.

4. Results

The nuclear surface extraction algorithm explained in the previous section was applied to a 47-level image stack of a developing *Arabidopsis* flower. As noted earlier, Figure 1a shows an *Amira* volume rendering of a CLSM image stack. In Figure 1b, the original green channel, which shows the nuclei, was removed; the 3D nuclear surfaces recovered by the algorithm were then superimposed with the red channel of the CLSM image stack yielding the volume rendering shown. Although we have not quantified the level of agreement between the true nuclei and the extracted model, the result, at least visually, is quite satisfying. Figure 1c shows the extracted surface mesh for a single giant cell nucleus.

References

1. [1] Bowman, J.L. et al. *Development*, **119**, 721-743, (1993).
2. [2] Canny, J., *T-PAMI*, **8**, 679-698, (1986).
3. [3] Drews, G.N. et al., *Cell*, **65**, 991-1002, (1991).
4. [4] Jofuku, K.D. et al. *Plant Cell*, **6**, 1211-1225, (1994).
5. [5] Lindeberg, T., *IJCV*, **30:2**, 177-154, (1998).
6. [6] Mandel, M.A. et al. *Nature*, **360**, 273-277, (1992).
7. [7] Martin, D. et al.*NIPS*, **15**, (2002).
8. [8] Reddy, G.V. et al., *Development*, **131**, 4225-4237, (2004).
9. [9] Steger, C., *T-PAMI*, **20**, 113-119, (Feb 1998).

[3]Clockwise or counterclockwise.